Electronic Supplimental Information (ESI) for:

Benzoquinone, 1,4-naphthoquinone radical anions, and their didehydro derivatives: Electroanalytical and predicted negative ion photoelectron spectroscopic studies

Nolan J. White[1], Wyatt W. Tunstall[1,2], Lucia A. Vargas, Kie T. Workman[1,2], Jonathan Moldenhauer[1] and Wilson K. Gichuhi[1]

[1]Department of Chemistry and [2]Department of Chemical Engineering, Tennessee Tech University, 1 William L Jones Dr., Cookeville, TN 38505.

1. Relationship between half-wave reduction potential and adiabatic EAs

The relationship between the solution half-wave reduction potential for the first half-wave reduction reaction in a given quinone molecule, its gas-phase adiabatic electron affinity, and the energy difference between the neutral quinone and its negative ion in the gas- and solution-phase, $\Delta\Delta G_{Solv}$, is given by equation S$_{1,}$

$$E_{1/2} = EA - \Delta\Delta G_{solv} + E_{ref}\,, \qquad \text{(S1)}$$

where E_{ref} is the voltage from the Ag^{+}/Ag reference electrode, EA the experimentally determined value of adiabatic electron affinity (EA), and $E_{1/2}$ the experimental half-wave reduction potential. If the value of $\Delta\Delta G_{Solv}$ for a given quinone molecule is known, the gas-phase adiabatic EA can be determined based on the recorded reversible half-wave reduction potential or vice versa. In principle, $\Delta\Delta G_{Solv}$ values depend on the degree of charge delocalization and molecules with similar localized or delocalized anionic charges are characterized by similar $\Delta\Delta G_{Solv}$.[1] It is therefore reasonable to utilize an average value $\Delta\Delta G_{Solv}$ in modelling either EAs or half-wave reduction potentials for a given homologous group of compounds based on their structural and chemical similarities.

If the $\Delta\Delta G_{solv}$ values and the experimental half-wave reduction potentials are known, one can utilize the relationship given in equation S1 obtain obtain corrected or standardized (i.e. corrected for stabilization due to solvation) half-wave reduction potentials ($E_{1/2\ Corrected}$), hence acquire a more accurate correlation between the solution half-wave reduction potentials and the calculated adiabatic electron affinities (EAs) for a group of similar molecules to benchmark the theoretically determined EA values. Armed with a carefully benchmarked theoretical protocol for adiabatic EAs allows one to extend the discussion on the origin 0-0 electron detachment peaks to other higher eBE features in a predicted photodetachment spectra reported in this work. These detachment features are signatures of the neutral vibrational structures and their intensities are governed by the Franck-Condon principle. Previously, the relationship between one-electron half-wave reduction potentials, hydride affinities, and Hammett substituent parameters in quinones was utilized to predict homolytic bond dissociation energies of hydroquinone anions.[2] The accurate prediction of adiabatic EAs are critical in elucidation of the nature of vibrational excitation in neutral quinone molecues following electron detachment from the gas-phase or solution-phase radical anions and dianions.

A comprehensive study on the correlation between gas-phase EAs and half-wave reduction potential by Ruoff et al. established that molecules with adiabatic EA values below ca. 2.0 eV tend to have $\Delta\Delta G_{Solv}$ values that varies from 1.9 eV to 2.75 eV.[1] According to Ruoff et al., the average $\Delta\Delta G_{Solv}$ for aromatic hydrocarbons, the most extensively studied group of compounds, is 1.99 eV. Ruoff et al. has provided a comprehensive guideline on how one can utilize the average values of $\Delta\Delta G_{Solv}$ for a group molecules, based on whether they have localized (Group C), partially localized (Group B), or delocalized (Group A) charge distributions, to obtain an accurate relationship between $E_{1/2\ Corrected}$ and adiabatic EAs to gain

insights into fundamental physical properties in molecules. Using the available experimental EA values for quinones, individual $\Delta\Delta G_{solv}$ were calculated and an average (2.68 eV) value obtained. Our $\Delta\Delta G_{solv}$values are slightly higher than the theoretical G3(MP2) values reported by Calbo et al.[3] In addition, our values are also sligtly higher than the obtained by Zhu and Wang using an integral equation formalism polarized continuum model (IEF-PCM) at the B3LYP/6-31+G** level (and using Bondi'S radii and gas-phase geometries).[2] It is reasonable to utilize a standardized $\Delta\Delta G_{solv}$ for the quinones molecules studied here based on their similar delocailzed charge distribution as revealed by the calculated molecular orbitals. Consequently, the average $\Delta\Delta G_{solv}$ was used for the calculation of $E_{1/2\ Corr}$ based on equation S2.

$$E_{1/2\ Corr} = EA - \Delta\Delta G_{solv\ avg} + E_{ref} \quad \text{(S2)}$$

Listed in Table S1 are the $\Delta\Delta G_{solv}$ (eV) values for each quinone, experimental half-wave reduction potentials, $E_{1/2,}$ and the corrected half-wave reduction potentials for the selected quinones, $E_{1/2\ Corr}$, reported in this manuscript.

2. Thermodynamic cycle for a one-electron attachment process

Scheme S1 shows the thermodynamic cycle for a one-electron attachment reaction that captures the correlation between gas-phase adiabatic electron affinities and the solution-phase half-wave reduction potentials in quinones. The sheme allows one to analyze solvation effects and determine the difference in Gibbs free energy based on the initial reactants. According to Scheme S1, the difference in the relative energies of electron attachment in the gas-phase (ΔG_{gas}) and in solution-phase (ΔG_{Solv}) is equal to the difference in the Gibbs free energies of solvation for the neutral quinone (ΔG_{Solv} (Q)) and its radical anion ($\Delta\Delta G_{Sol}$ (Q^{-})). This relationship is given in Equation S3,

$$\Delta\Delta G_{Solv} = \Delta G_{red} - \Delta G_{gas} = \Delta G_{solv}\,(Q^{-}) - \Delta G_{solv}\,(Q). \quad \text{(S3)}$$

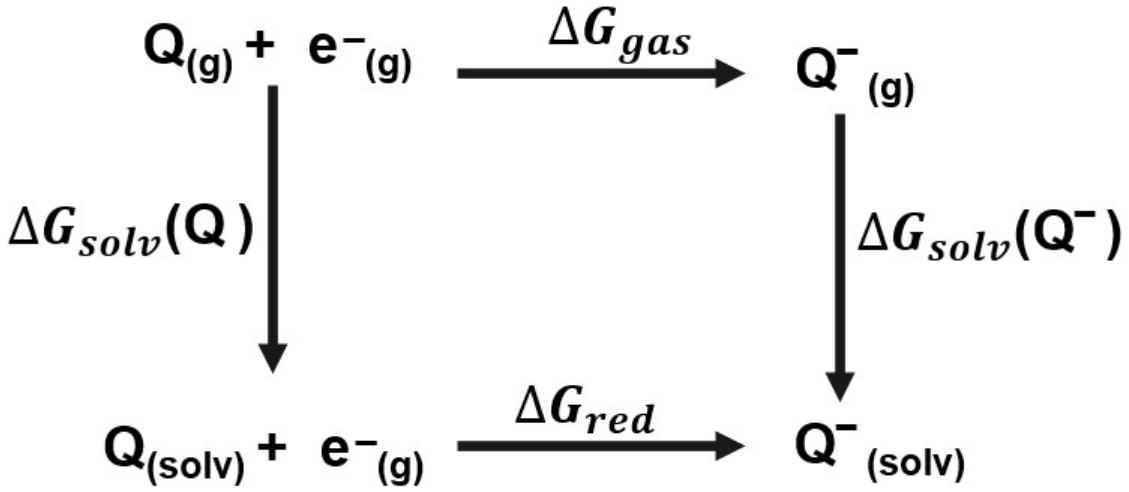

Scheme S1: A thermodynamic cycle for a one-electron attachment reaction showing the relationship between the standard Gibbs energy of the reaction in gas-phase to the standard Gibbs free energy of the reaction in the solution-phase.

Accordingly, the total change in Gibbs free energy for a one-electron attachment reaction in solution is related to the absolute value of the reduction potential, $E^{abs}{}_{1/2}$, as outlined in equation S4,

$$E^{abs}{}_{1/2} = \Delta G_{red/}(-nF), \quad \text{(S4)}$$

where n is the number of electrons transferred, which in this case is one and F is the Faraday constant (F = 96.5 kJ mol^{-1} V^{-1}). The ΔG_{red} term is given by equation S5,

$$\Delta G_{red} = \Delta G_{gas} + \Delta G_{solv}. \quad \text{(S5)}$$

From equation S3, one can re-write $E^{abs}{}_{1/2}$ in the form of Equation S6,

$$E^{abs}{}_{1/2} = -\Delta G_{gas} - \Delta\Delta G_{Solv}, \quad \text{(S6)}$$

where the ΔG_{gas} and $\Delta\Delta G_{Solv}$ are in eV and $E^{abs}{}_{1/2}$ is in V. The expression that relates the absolute first half-wave reduction potentials based on the thermodynamic cycle shown in Scheme S1, Equation S7, can now be written as equation S8.

$$E^{abs}{}_{1/2} = -(\Delta G_{gas} + RT.\ln 24.46) - \Delta\Delta G_{Solv}, \quad \text{(S7)}$$

$$E_{1/2} = E^{abs}{}_{1/2} - E_{ref} = -(\Delta G_{gas} - \Delta\Delta G_{Solv} - E_{ref}. \quad \text{(S8)}$$

In summary, Equations S6 and S8 allows one to relate the Gibbs free energy difference between the neutral and the anionic species in the gas-phase (ΔG_{gas}) with the half-wave reduction potential ($E_{1/2}$) based on the Gibbs free energy of solvation ($\Delta\Delta G_{Solv}$).

Summary of Figures and Tables:

List of Figs.

Fig. S1: Room temperature cyclic voltammograms (CV) for (a) *para*-benzoquinone (*p*-BQ), (b) 1,4-napthoquinone (1,4-NQ), (c) 9,10-anthraquinone (9,10-AQ), and (d**)** 1-chloro-9,10-anthraquinone (1Cl-9,10-AQ) in acetonitrile. Tetrabutylammonium hexafluorophosphate was present as the electrolyte with a scan rate of 0.10 (V/s).

Fig. S2: Room temperature cyclic voltammograms (CV) for (a) benzene, (b) naphthalene, and (c) anthracene in acetonitrile. Tetrabutylammonium hexafluorophosphate was present as the electrolyte with a scan rate of 0.10 (V/s)

Fig. S3: Plot of B3LYP 6-311g++(2d,2p) gas-phase electron affinity values versus the first condensed-phase reduction potentials of benzene; *p*-BQ, 2,3-didehydro-*p*-BQ, naphthalene; 1,4-NQ, 2,3-didehydro-1,4-NQ, anthracene, 9,10-AQ, and 1Cl-9,10-AQ.

Fig. S4: The optimized geometries of *p*-BQ and 1,4-NQ radical anions and neutrals. Numbering is used to describe geometry changes between the anion and the neutral singlet state, following electron detachment from the initial doublet anionic state. The major changes in bond lengths and angles in each case are indicated in the Figure. The molecules listed in the Figure are as follows: (a) *p*-BQ anion; (b) *p*-BQ singlet; (c) *p*-BQ lowest-lying triplet state (T_1); (d) 1,4-NQ anion, (e) 1,4-NQ singlet; and (f) 1,4-NQ T_1. The geometries were optimized at the B3LYP 6-311g++(2d,2p) and B3LYP/aug-cc-pVQZ level of theories using a Gaussian 09 computational package.[4] Only the B3LYP/aug-cc-pVQZ values are shown.

Fig. S5: The optimized geometries of 2,3-didehydro-*p*-BQ, and 2,3-didehydro-1,4-NQ radical anions with their corresponding neutrals. Numbering is used to describe geometry change between the anion and the neutral singlet state, following electron photodetachment. The molecules are listed in the Figure as follows: (a) 2,3-DD-*p*-BQ anion, (b) 2,3-DD-*p*-BQ S_0, (c) 2,3-DD-*p*-BQ T_1; (d) 2,3-DD-1,4-NQ anion; (e) 2,3-DD-1,4-NQ S_0, and (f) 2,3-DD-1,4-NQ T_1. The geometries were optimized at the B3LYP 6-311g++(2d,2p) and B3LYP/aug-cc-pVQZ levels. Only the B3LYP/aug-cc-pVQZ values are shown.

Fig. S6: B3LYP 6-311g++(2d,2p) optimized geometries for (a) benzene, (b) naphthalene, and (c) anthracene radical anions together with their neutrals with numbering used to describe geometry changes between the anion and the neutral singlet states following electron detachment from the initial neutral state.

Fig. S7: B3LYP 6-311g++(2d,2p) optimized geometries of (a) 1,2-didehydrobenzene (1,2-DD-Bz), (b) 1,3-didehydrobenzene (1,3-DD-Bz), and (c)1,4-didehydrobenzene (1,4-DD-Bz) radical anions together with their neutrals with numbering used to describe geometry changes between the anion and the neutral singlet state following electron detachment from the initial state.

Fig. S8: B3LYP 6-311g++(2d,2p) optimized geometries of (a) 1,2-didehydronapthalene (1,2-DD-Nh) and (b)1,3-didehydronapthalene (1,3-DD-Nh) with numbering used to describe geometry changes between the anion and the neutral singlet state following electron detachment from the initial state.

Fig. S9: Mulliken atomic charges of the (a) *p*-BQ; (b) 2,3-DD-*p*-BQ; (c) 1,4-NQ; and (d) 2,3-DD-1,4-NQ doublet anion ground states. Only the B3LYP/aug-cc-pVQZ results are shown.

Fig. S10 (a) Singly occupied molecular orbital (SOMO) and (b) lowest unoccupied molecular orbital (LUMO) for *p*-BQ . The SOMO and LUMO for 1,4-NQ radical anions are shown in (c) and (d), respectively.

Fig. S11 (a) SOMO and (b) LUMO for 2,3-DD-*p*-BQ radical anions. The ones for the 2,3-DD-1,4-NQ radical anions are shown in (c), and (d).

Fig. S12: Primary Franck-Condon (FC) active normal vibrational modes, following electron detachment from the 2,3-DD-*p*-BQ radical anions to the corresponding T_1 neutral state as discussed in the main text. Each eigenvector shown here is that of the neutral molecule at the B3LYP/6-311g++(2d,2p) level of theory.

Fig. S13 (a) and (b): Primary FC-active normal vibrational modes for electron detachment from *p*-BQ radical anions to corresponding neutral S_0 and T_1 neutral states as discussed in the main

text. Each eigenvector shown here is that of the neutral molecule at the B3LYP/6-311g++(2d,2p) level of theory.

Fig. S14 (a) and (b): Primary FC-active normal vibrational modes for electron detachment from 1,4-NQ radical anions to corresponding neutral S_0 and T_1 neutral states as discussed in the main text. Each eigenvector shown here is that of the neutral molecule at the B3LYP/6-311g++(2d,2p) level of theory.

Fig. S15: Primary FC-active normal vibrational modes for electron detachment from 2,3-DD-1,4-NQ radical anions to the corresponding neutral S_0 state as discussed in the main text. Each eigenvector shown here is that of the neutral molecule at the B3LYP/6-311g++(2d,2p) level of theory.

List of Tables

Table S12: B3LYP/6-311g++(2d,2p) interatomic bond lengths (Å) and bond angles (deg.) for 1,2-DD-Nh radical anions and the corresponding neutral S_0 and T_1 states. The major changes in bond lengths are shown in red

Table S13: Calculated dipole moments for the *p*-BQ, 2,3-DD-*p*-BQ, 1,4-NQ, and 2,3-DD-1,4-NQ radical anions. Only the B3LYP/6-311g++(2d,2p) results are shown.

Table S14: Normal harmonic vibrational modes (ν_1 to ν_{24}) for the anion, neutral singlet and the T_1 state in 2,3-didehydro-*p*-BQ.

Table S15: Normal harmonic vibrational modes (ν_1 to ν_{30}) for the anion, neutral singlet and the T_1 state in *p*-BQ.

Table S16: Normal harmonic vibrational modes (ν_1 to ν_{48}) for the anion, neutral singlet and the T_1 state in 1,4-NQ.

Table S17: Normal harmonic vibrational modes (ν_1 to ν_{42}) for the anion, neutral singlet and T_1 state in 2,3-didehydro-1,4-NQ.

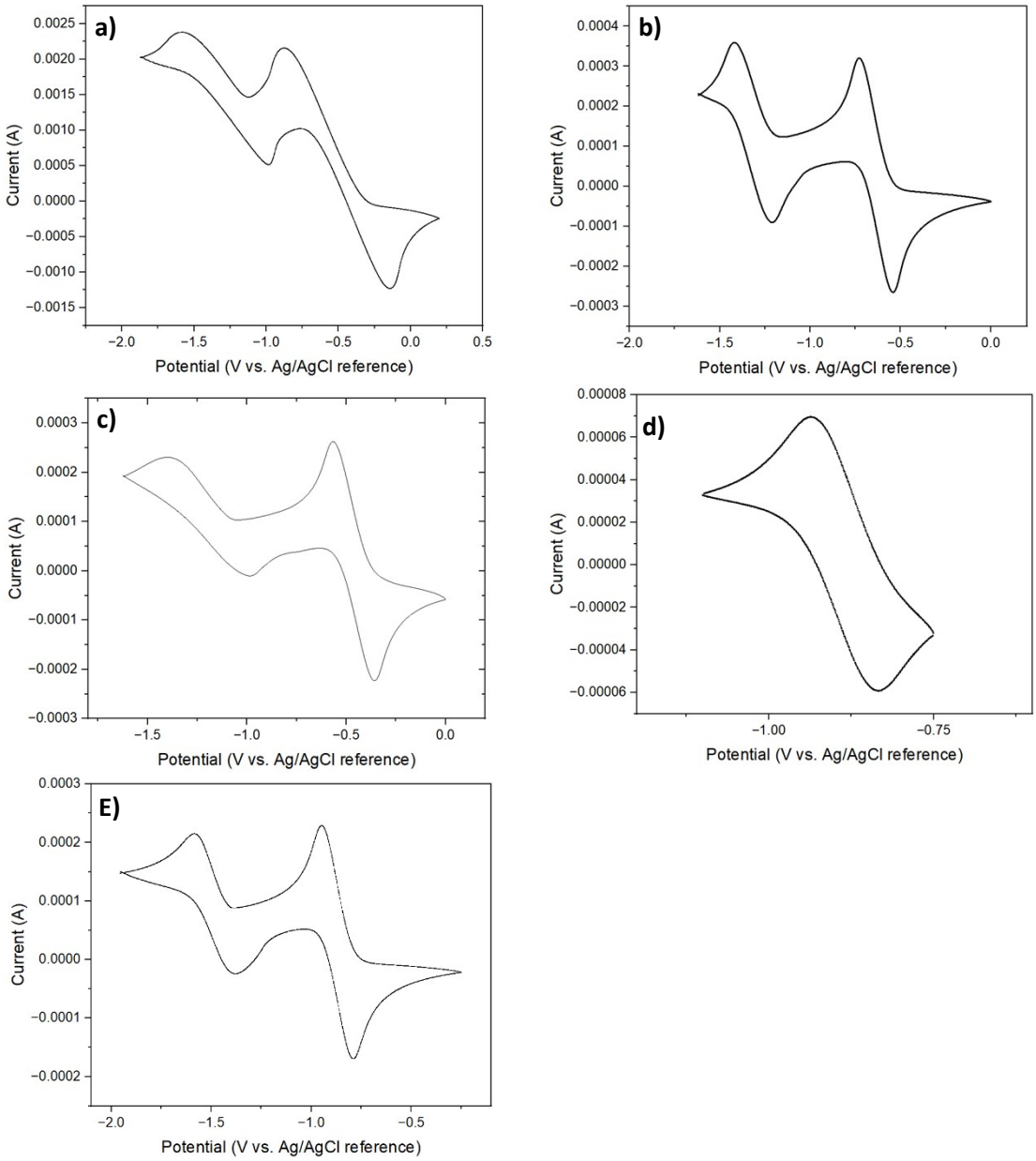

Fig. S1: Room temperature cyclic voltammograms (CV) for (a) *p*-BQ, (b)1,4-NQ, (c) 1,2-NQ, d) 9,10-AQ, and e)1-Cl-9,10-AQ in acetonitrile. Tetrabutylammonium hexafluorophosphate was present as the electrolyte, and the scan rate was fixed at 0.10 (V/s).

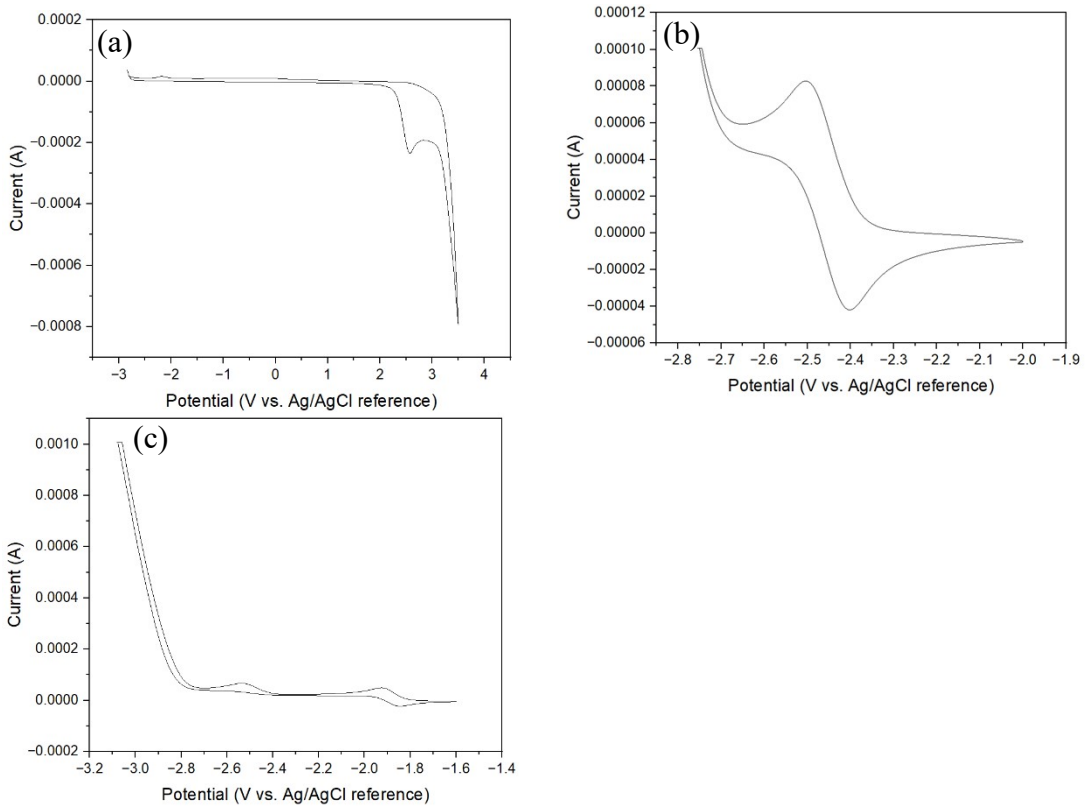

Fig. S2: Room temperature cyclic voltammograms (CV) for (a) benzene, (b) naphthalene, and (c) anthracene in acetonitrile. Tetrabutylammonium hexafluorophosphate was present as the electrolyte, and the scan rate was fixed at 0.10 (V/s).

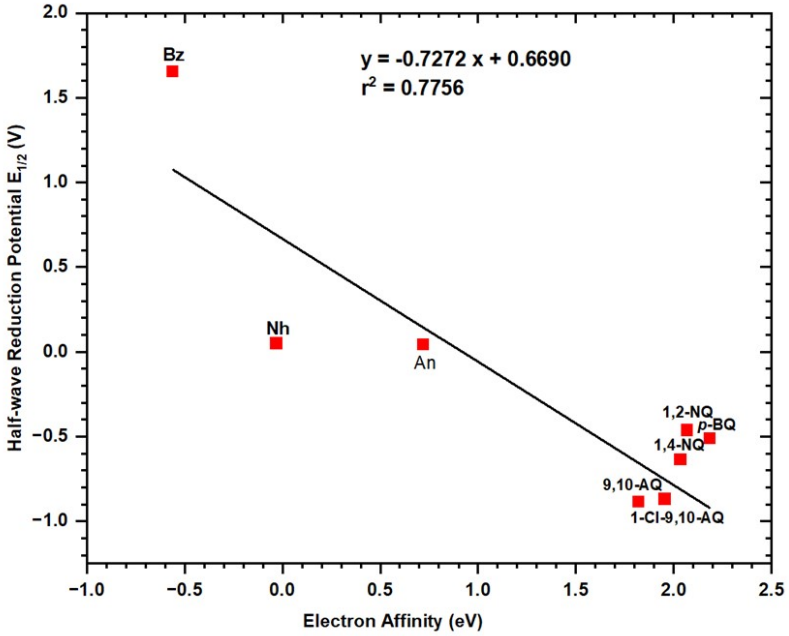

Fig. S3: Plot of B3LYP 6-311g++(2d,2p) gas-phase electron affinity values versus the first condensed-phase half-wave reduction potentials for: benzene(Bz), *p*-BQ, naphthalene (Nh), 1,4-NQ, 1,4-NQ, anthracene (An), 9,10-AQ, and 1Cl-9,10-AQ.

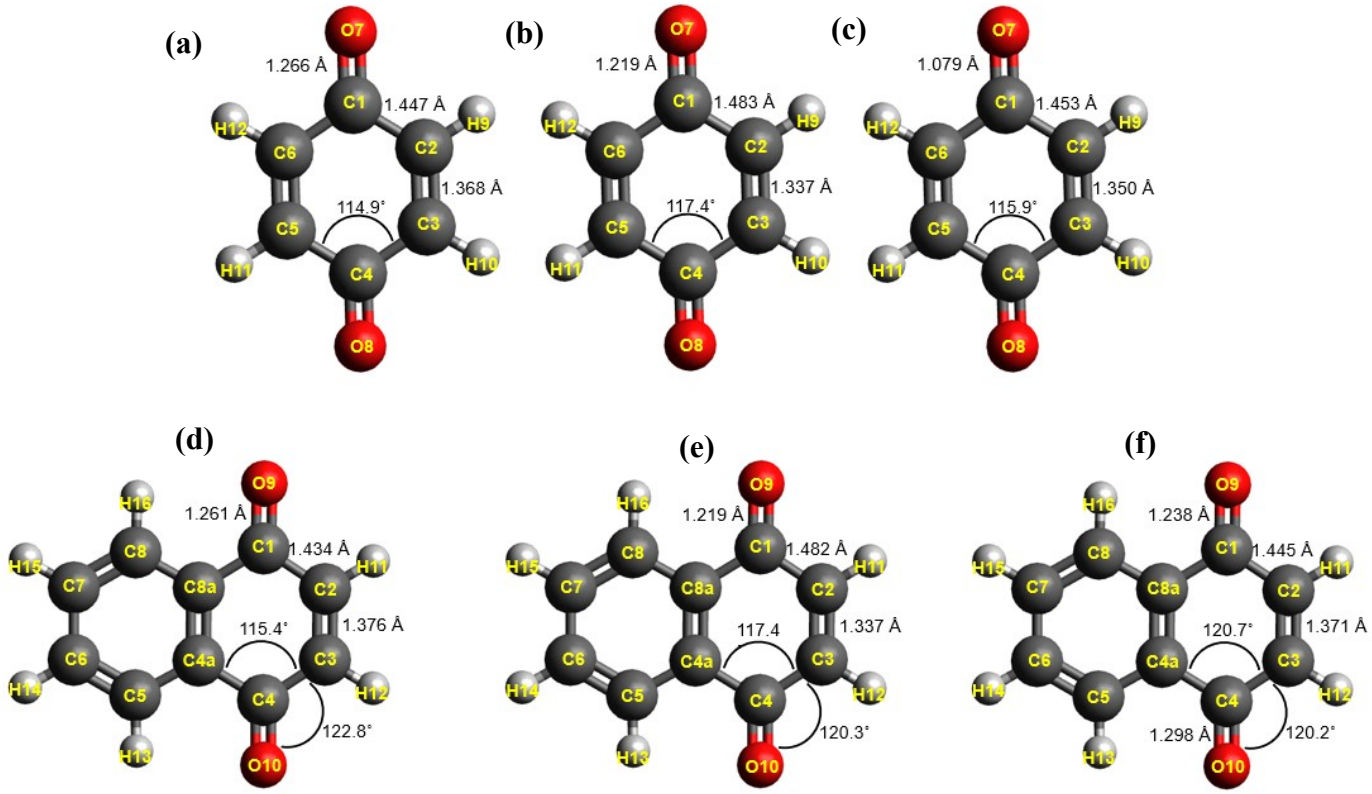

Fig. S4: The optimized geometries of *p*-BQ and 1,4-NQ radical anions and neutrals. Numbering is used to describe geometry changes between the anion and the neutral singlet state, following electron detachment from the initial doublet anionic state. The major changes in bond lengths and angles in each case are indicated in the Figure. The molecules listed in the Figure are as follows: (a) *p*-BQ anion; (b) *p*-BQ singlet; (c) *p*-BQ lowest-lying triplet state (T_1); (d) 1,4-NQ anion, (e) 1,4-NQ singlet; and (f) 1,4-NQ T_1. The geometries were optimized at the B3LYP 6-311g++(2d,2p) and B3LYP/aug-cc-pVQZ level of theories using a Gaussian 09 computational package.[4] Only the B3LYP/aug-cc-pVQZ values are shown.

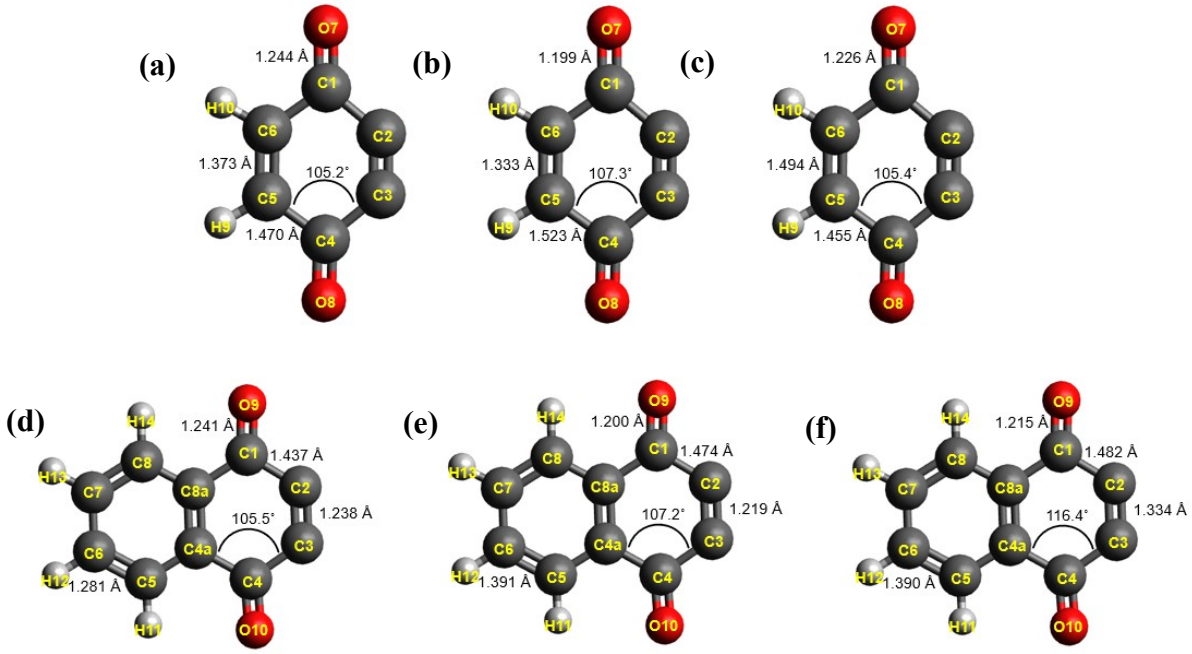

Fig. S5: The optimized geometries of 2,3-didehydro-*p*-BQ, and 2,3-didehydro-1,4-NQ radical anions with their corresponding neutrals. Numbering is used to describe geometry change between the anion and the neutral singlet state, following electron photodetachment. The molecules are listed in the Figure as follows: (a) 2,3-DD-*p*-BQ anion, (b) 2,3-DD-*p*-BQ S_0, (c) 2,3-DD-*p*-BQ T_1; (d) 2,3-DD-1,4-NQ anion; (e) 2,3-DD-1,4-NQ S_0, and (f) 2,3-DD-1,4-NQ T_1. The geometries were optimized at the B3LYP 6-311g++(2d,2p) and B3LYP/aug-cc-pVQZ levels. Only the B3LYP/aug-cc-pVQZ values are shown.

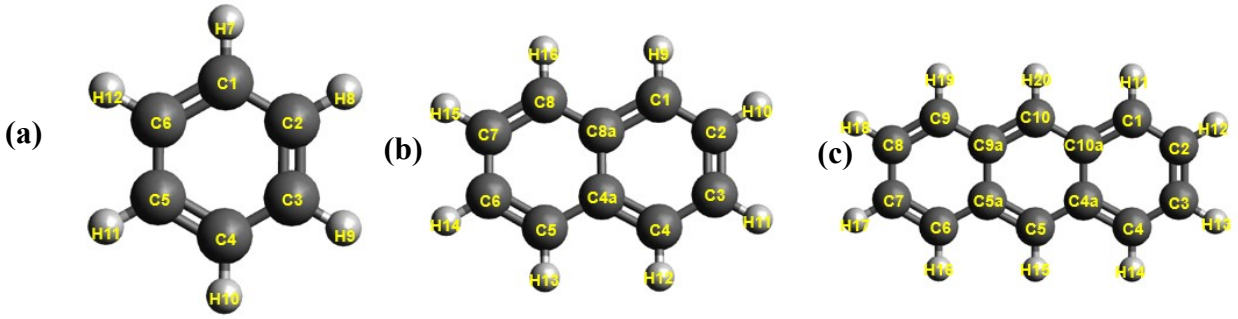

Fig. S6: B3LYP 6-311g++(2d,2p) optimized geometries for (a) benzene, (b) naphthalene, and (c) anthracene radical anions together with their neutrals with numbering used to describe geometry changes between the anion and the neutral singlet states following electron detachment from the initial neutral state.

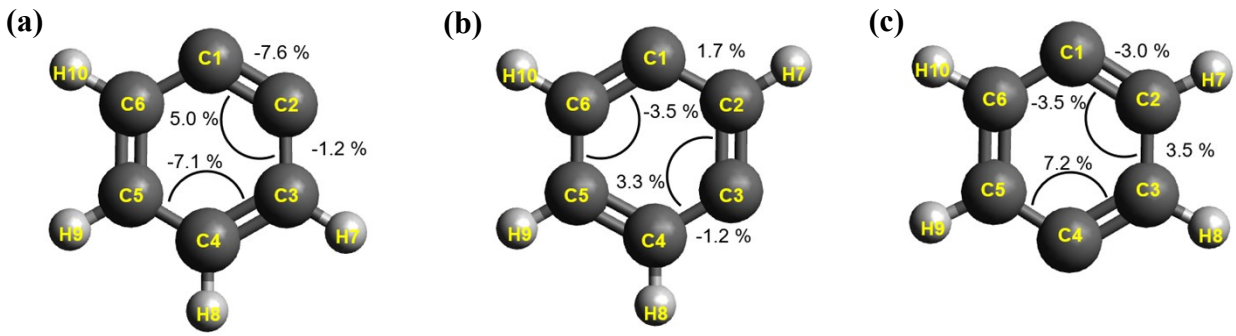

Fig. S7: B3LYP 6-311g++(2d,2p) optimized geometries of (a) 1,2-didehydrobenzene(1,2-DD-Bz), (b) 1,3-didehydrobenzene (1,3-DD-Bz), and (c) 1,4-didehydrobenzene (1,4-DD-Bz) radical anions together with their neutrals with numbering used to describe geometry changes between the anion and the neutral singlet state following electron detachment from the initial state.

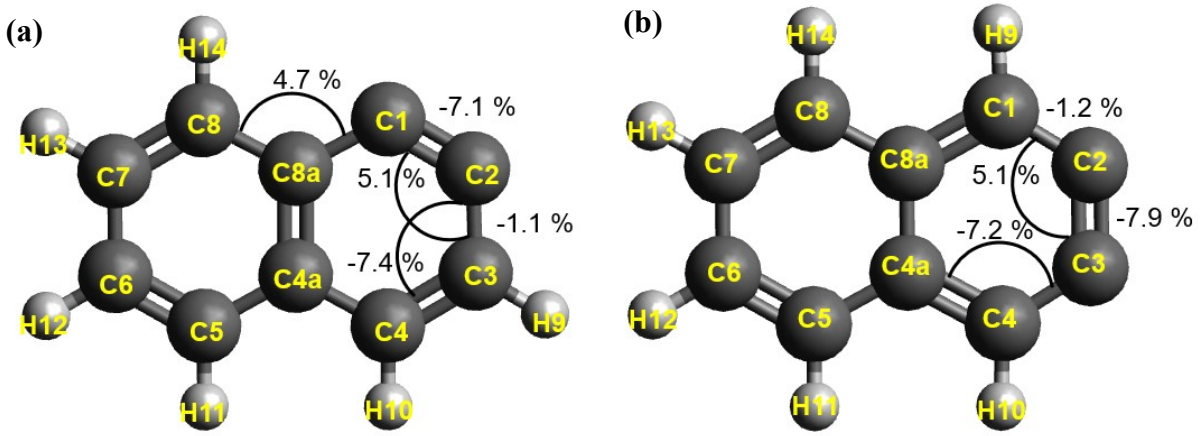

Fig. S8: B3LYP 6-311g++(2d,2p) optimized geometries of (a) 1,2-didehydronapthalene (1,2-DD-Nh) and (b)1,3-didehydronapthalene (1,3-DD-Nh) with numbering used to describe geometry changes between the anion and the neutral singlet state following electron detachment from the initial state. The major changes in geometry (shown as %) from the anion to the S_0 states are indicated in the Figures.

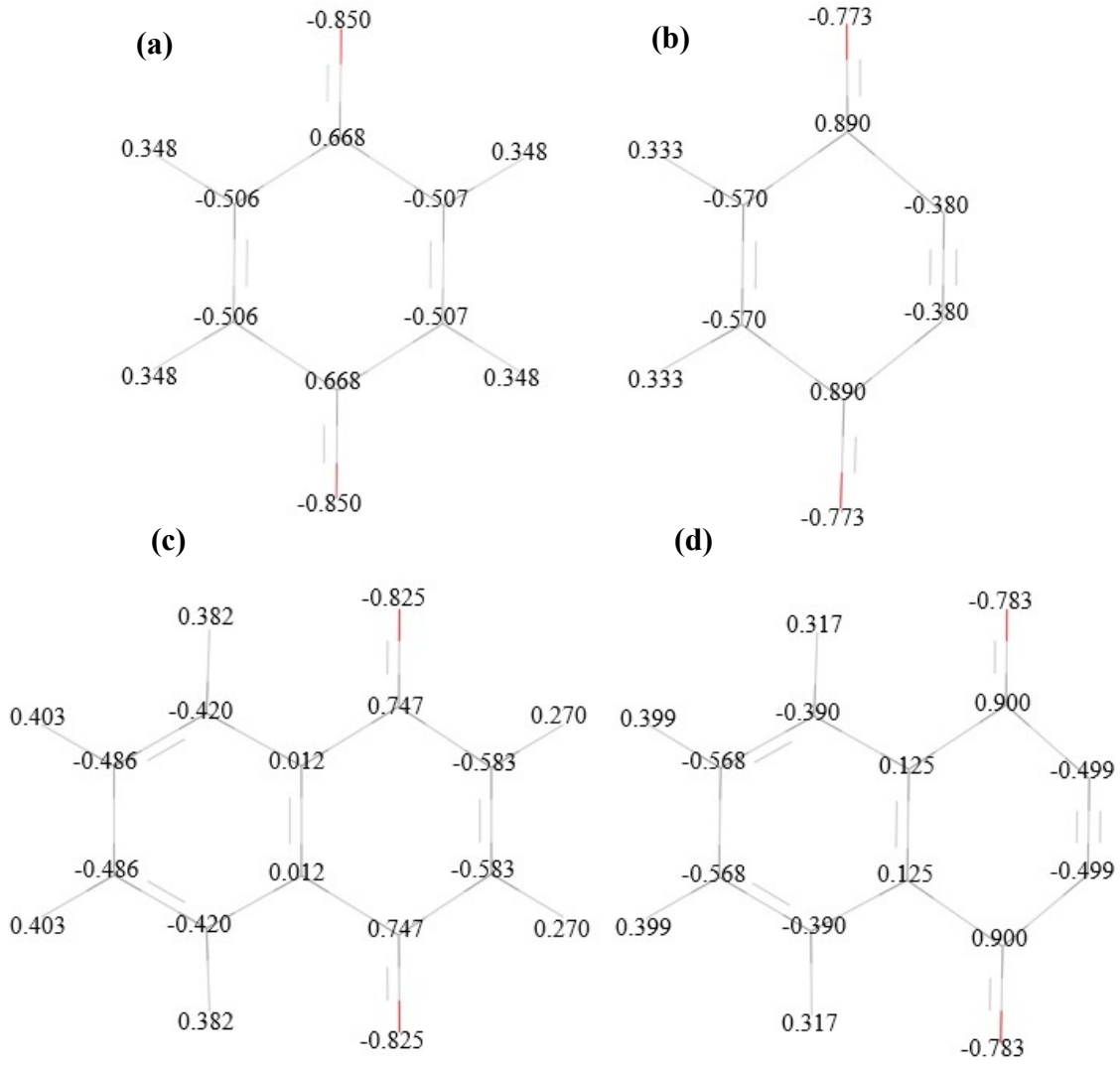

Fig. S9: Mulliken atomic charges for the (a) *p*-BQ, (b) 2,3-DD-*p*-BQ, (c) 1,4-NQ, and (d) 2,3-DD-1,4-NQ doublet anion ground states. Only the B3LYP/aug-cc-pVQZ results are shown.

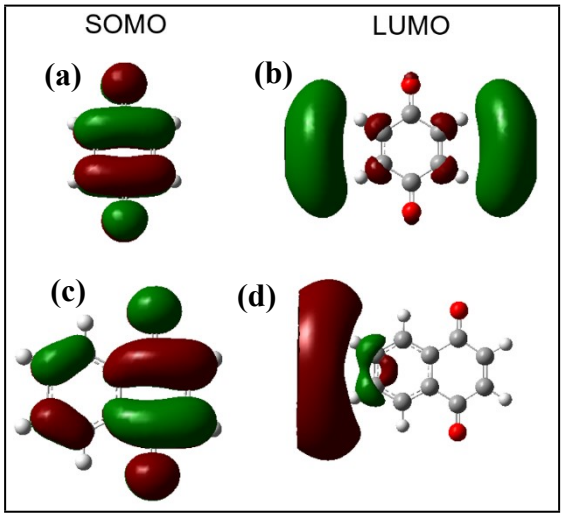

Fig. S10 (a) SOMO and (b) LUMO for *p*-BQ. The ones for 1,4-NQ radical anions are shown in (c) and (d).

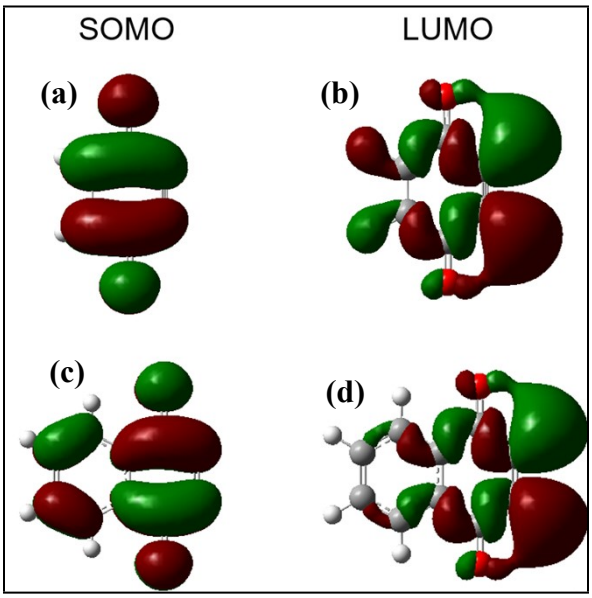

Fig. S11 (a) SOMO and (b) LUMO for 2,3-DD-*p*-BQ. The ones for 2,3-DD-1,4-NQ radical anions are shown in (c), and (d).

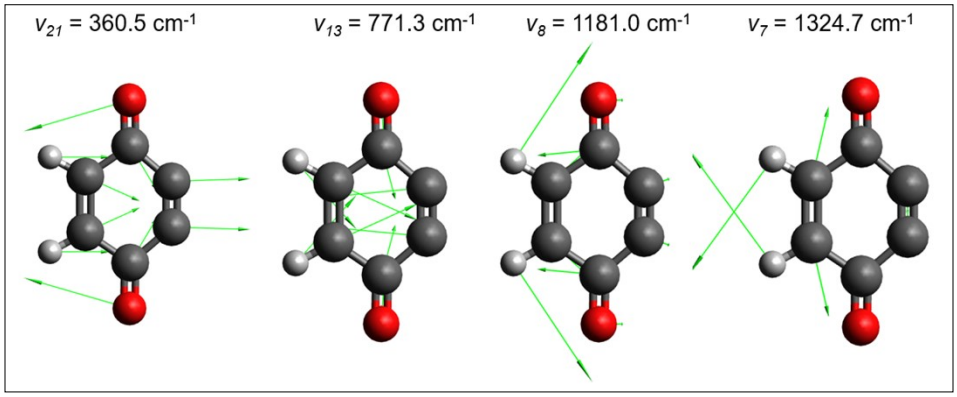

Fig. S12: Primary FC active normal vibrational modes for electron detachment from 2,3-DD-*p*-BQ radical anions to the corresponding T_1 neutral state as discussed in the main text. Each eigenvector shown here is that of the neutral molecule.

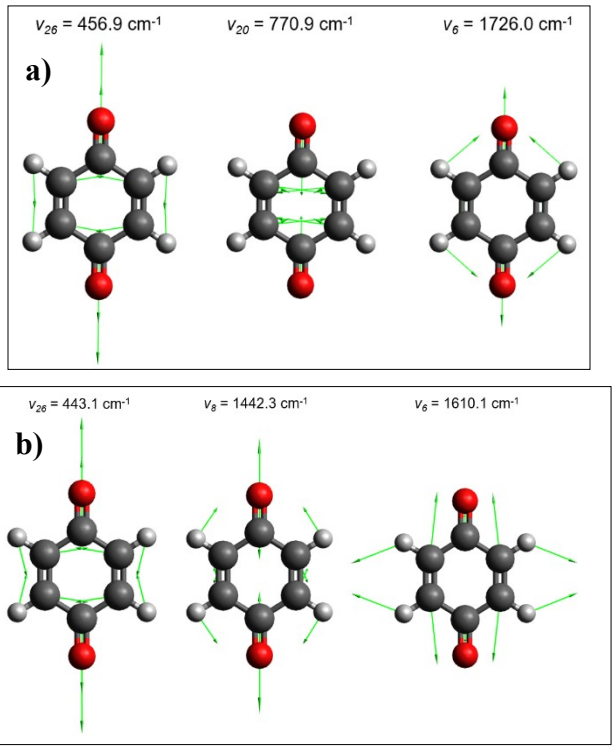

Fig. S13 (a) and (b): Primary FC active normal modes for electron detachment from *p*-BQ radical anions to corresponding neutral S_0 and T_1 neutral states as discussed in the main text. Each eigenvector shown here is that of the neutral molecule.

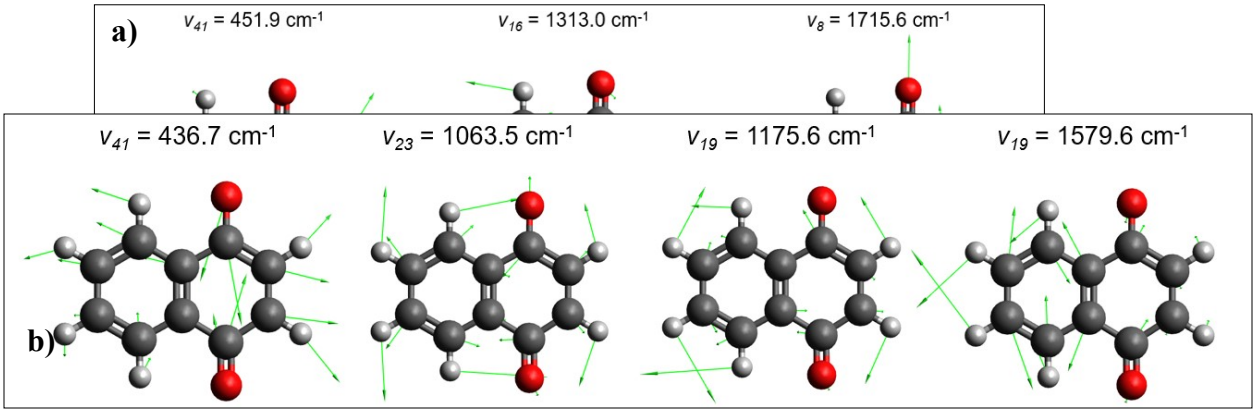

Fig. S14 (a) and (b): Primary FC active normal modes for electron detachment from 1,4-NQ radical anions to corresponding neutral S_0 and T_1 neutral states as discussed in the main text. Each eigenvector shown here is that of the neutral molecule.

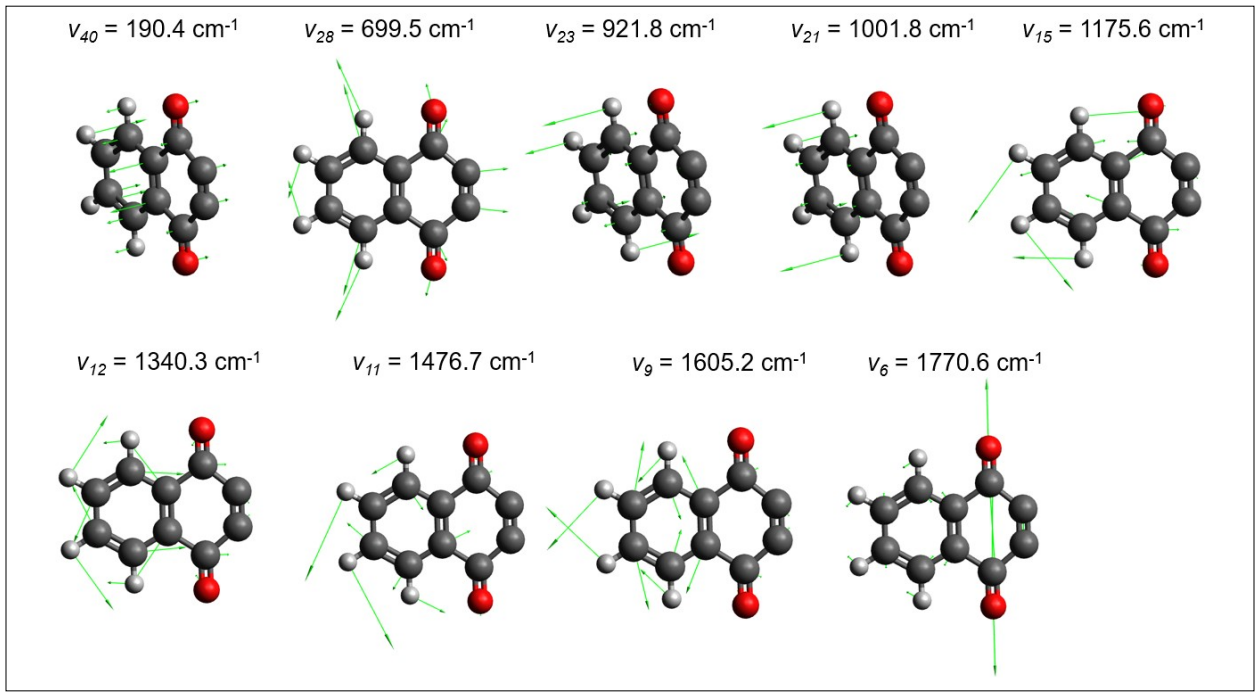

Fig. S15: Primary FC active normal modes for electron detachment from 2,3-DD-1,4-NQ radical anions to corresponding neutral S_0 as discussed in the main text. Each eigenvector shown here is that of the neutral molecule.

List of Tables

Table S1: Values of $\Delta\Delta G_{solv}$ (eV) values, experimental half-wave reduction potentials, $E_{1/2}$, and the corrected half-wave reduction potentials, $E_{1/2corrected}$ for the quinones studied.

Quinone	$\Delta\Delta G_{solv}$ (eV)	$E_{1/2}$ (experimental) V	$E_{1/2corrected}$ V
p-benzoquinone	2.594 ± 0.009	-0.51130 ± 0.0707	-0.6061 ± 0.1000
1,4-naphthoquinone	2.662 ± 0.049	-0.6355 ± 0.0707	-0.6621 ± 0.1108
1,2-naphthoquinone	2.458 ± 0.007**	-0.4620 ± 0.0707	-0.6921 ± 0.0999
9,10-anthraquinone	2.699 ± 0.061	-0.8854 ± 0.0707	-0.8751 ± 0.1170
1-Cl-9,10-anthraquionone	2.800 ± 0.061	-0.8685 ± 0.0707	-0.7571 ± 0.1170
$\Delta\Delta G_{solv}$ average	2.689 ± 0.0999		

***Value calculated using the electron affinity calculated at the B3LYP/6-311g(2d,2p) level of theory; excluded from the $\Delta\Delta G_{solv}$ average.*

Table S2: Calculated interatomic bond lengths (Å), bond angles (deg.) for the *p*-BQ radical anions to corresponding neutral S_0 and T_1 neutral states. The major changes in bond length are shown in red.

	Singlet	Anion		Triplet	
C-C Bond			% Change		% Change
C1-C2	1.483	1.447	2.5	1.453	0.4
C2-C3	1.337	1.368	-2.3	1.350	-1.3
C3-C4	1.483	1.447	2.5	1.453	0.4
C4-C5	1.483	1.447	2.5	1.453	0.4
C5-C6	1.337	1.368	-2.3	1.350	-1.3
C6-C1	1.483	1.447	2.5	1.453	0.4
C-H Bond					
C2-H9	1.082	1.084	-0.2	1.079	-0.5
C3-H10	1.082	1.084	-0.2	1.079	-0.5
C5-H11	1.082	1.084	-0.2	1.079	-0.5
C6-H12	1.082	1.084	-0.2	1.079	-0.5
C=O Bond					

C1=O7	1.219	1.266	-3.7	1.251	-1.2
C4=O8	1.219	1.266	-3.7	1.251	-1.2

	Singlet	Anion		Triplet	
C-C-C Angle			% Change		% Change
C1-C2-C3	121.3	122.5	-1.0	122.0	-0.4
C2-C3-C4	121.3	122.5	-1.0	122.0	-0.4
C3-C4-C5	117.4	114.9	2.1	115.9	0.9
C4-C5-C6	121.3	122.5	-1.0	122.0	-0.4
C5-C6-C1	121.3	122.5	-1.0	122.0	-0.4
C6-C1-C2	117.4	114.9	2.1	115.9	0.9
C-C-H Angle					
C1-C2-H9	116.0	116.5	-0.4	116.3	-0.2
C3-C2-H9	122.8	121.0	1.5	121.6	0.5
C2-C3-H10	122.8	121.0	1.5	121.6	0.5
C4-C3-H10	116.0	116.5	-0.4	116.3	-0.2
C4-C5-H11	116.0	116.5	-0.4	116.3	-0.2
C6-C5-H11	122.8	121.0	1.5	121.6	0.5
C5-C6-H12	122.8	121.0	1.5	121.6	0.5
C1-C6-H12	116.0	116.5	-0.4	116.3	-0.2
C-C=O Angle					
C2-C1-O7	121.3	122.5	-1.0	122.0	-0.4
C6-C1-O7	121.3	122.5	-1.0	122.0	-0.4
C3-C4-O8	121.3	122.5	-1.0	122.0	-0.4
C5-C4-O8	121.3	122.5	-1.0	122.0	-0.4

Table S3: Calculated interatomic bond lengths (Å), bond angles (deg.) for the 2,3-DD-*p*-BQ radical anions to corresponding neutral S_0 and T_1 neutral states. The major changes in bond length are shown in red. Only the B3LYP/6-311g++(2d,2p) results are shown.

	Singlet	Anion		Triplet	
C-C Bond			% Change		% Change
C1-C2	1.477	1.457	1.4	1.464	0.5
C2-C3	1.221	1.236	-1.2	1.226	-0.8
C3-C4	1.477	1.457	1.4	1.464	0.5
C4-C5	1.523	1.470	3.6	1.455	-1.0
C5-C6	1.333	1.373	-2.9	1.494	8.8
C6-C1	1.523	1.470	3.6	1.455	1.0
C-H Bond					
C5-H9	1.082	1.084	-0.2	1.082	-0.2
C6-H10	1.082	1.084	-0.2	1.082	-0.2

C=O Bond					
C1=O7	1.199	1.244	-3.6	1.226	-1.4
C4=O8	1.199	1.244	-3.6	1.226	-1.4

	Singlet	Anion		Triplet	
C-C-C Angle			% Change		% Change
C1-C2-C3	128.3	129.3	-0.8	130.5	0.9
C2-C3-C4	128.3	129.3	-0.8	130.5	0.9
C3-C4-C5	107.3	105.2	2.0	105.4	0.2
C4-C5-C6	124.4	125.5	-0.9	124.1	-1.1
C5-C6-C1	124.4	125.5	-0.9	124.1	-1.1
C6-C1-C2	107.3	105.2	2.0	105.4	0.2
C-C-H Angle					
C4-C5-H9	113.9	114.7	-0.7	117.1	2.1
C6-C5-H9	121.8	119.8	1.7	118.8	-0.8
C5-C6-H10	121.8	119.8	1.7	118.8	-0.8
C1-C6-H10	113.9	114.7	-0.7	117.1	2.1
C-C=O Angle					
C2-C1-O7	130.2	130.3	-0.1	131.4	0.8
C6-C1-O7	122.5	124.5	-1.6	123.2	-1.0
C3-C4-O8	130.2	130.3	-0.1	131.4	0.8
C5-C4-O8	122.5	124.5	-1.6	123.2	-1.0

Table S4: Calculated interatomic bond lengths (Å), bond angles (deg.) for the 1,4-NQ radical anions and the corresponding neutral S_0 and T_1 neutral states. The major changes in bond length are shown in red. Only the B3LYP/6-311g++(2d,2p) results are shown.

	Singlet	Anion		Triplet	
C-C Bond			% Change		% Change
C1-C2	1.482	1.434	3.3	1.445	0.8
C2-C3	1.337	1.376	-2.8	1.371	-0.4
C3-C4	1.482	1.434	3.3	1.415	-1.3
C4-C4a	1.490	1.475	1.0	1.453	-1.5
C4a-C5	1.394	1.406	-0.9	1.408	0.1
C5-C6	1.388	1.381	0.5	1.379	-0.1
C6-C7	1.395	1.406	-0.8	1.402	-0.3
C7-C8	1.388	1.381	0.5	1.382	0.1
C8-C9	1.394	1.406	-0.9	1.400	-0.4
C8a-C1	1.490	1.475	1.0	1.481	0.4
C8a-C4a	1.404	1.420	-1.1	1.409	-0.8

C-H Bond					
C2-H11	1.082	1.084	-0.2	1.081	-0.3
C3-H12	1.082	1.084	-0.2	1.079	-0.5
C5-H13	1.080	1.082	-0.2	1.081	-0.1
C6-H14	1.081	1.084	-0.3	1.081	-0.3
C7-H15	1.081	1.084	-0.3	1.081	-0.3
C8-H16	1.080	1.082	-0.2	1.081	-0.1
C=O Bond					
C1=O9	1.219	1.261	-3.3	1.238	-1.8
C4=O10	1.219	1.261	-3.3	1.298	2.9

	Singlet	Anion		Triplet	
C-C-C Angle			% Change		% Change
C1-C2-C3	122.2	123.3	-0.9	123.0	-0.2
C2-C3-C4	122.2	123.3	-0.9	120.5	-2.3
C3-C4-C4a	117.4	115.4	1.7	120.7	4.6
C4-C4a-C8a	120.5	121.3	-0.7	118.4	-2.4
C4-C4a-C5	119.7	119.7	0	121.4	1.4
C4a-C8a-C1	120.4	121.3	-0.7	121.5	0.2
C4a-C5-C6	120.0	121.1	-0.9	119.8	-1.1
C5-C6-C7	120.2	119.9	0.3	120.3	0.3
C6-C7-C8	120.2	119.9	0.3	120.2	0.3
C7-C8-C8a	120.0	121.1	-0.9	120.8	-0.2
C8-C8a-C1	119.7	119.7	0	119.7	0
C8-C8a-C4a	119.8	119.0	0.7	118.8	-0.2
C8a-C4a-C4	120.4	121.3	-0.7	118.4	-2.4
C8a-C4a-C5	119.8	119.0	0.7	120.2	1.0
C8a-C1-C2	117.4	115.4	1.7	116.0	0.5
C-C-H Angle					
C1-C2-H11	115.5	116.2	-0.6	116.8	0.5
C3-C2-H11	122.3	120.5	1.5	120.2	-0.2
C2-C3-H12	122.3	120.5	1.5	121.6	0.9
C4-C3-H12	115.5	116.2	-0.6	117.9	1.5
C4a-C5-H13	118.7	117.4	1.1	119.7	2.0
C6-C5-H13	121.3	121.5	-0.2	120.6	-0.7
C5-C6-H14	119.9	120.1	-0.2	119.7	-0.3
C7-C6-H14	119.9	120.0	-0.1	120.0	0.0
C6-C7-H15	119.9	120.0	-0.1	119.9	-0.1
C8-C7-H15	119.9	120.1	-0.2	120.0	-0.1
C7-C8-H16	121.3	121.5	-0.2	121.7	0.2
C8a-C8-H16	118.7	117.4	1.1	117.6	0.2

C-C=O Angle					
C2-C1-O9	120.3	122.8	-2.0	122.2	-0.5
C8a-C1-O0	122.3	121.8	0.4	121.8	0.0
C3-C4-O10	120.3	122.8	-2.0	120.2	-2.1
C4a-C4-O10	122.3	121.8	0.4	119.1	-2.2

Table S5: Calculated interatomic bond lengths (Å), bond angles (deg.) for the 2,3-DD-1,4-NQ radical anions to the corresponding neutral S_0 and T_1 neutral states. The major changes in bond length are shown in red. Only the B3LYP/6-311g++(2d,2p) results are shown.

	Singlet	Anion		Triplet	
C-C Bond			% Change		% Change
C1-C2	1.474	1.437	2.6	1.482	3.1
C2-C3	1.219	1.238	-1.5	1.334	7.7
C3-C4	1.474	1.437	2.6	1.482	3.1
C4-C4a	1.529	1.503	1.7	1.495	-0.5
C4a-C5	1.392	1.407	-1.1	1.393	-1.0
C5-C6	1.391	1.281	8.6	1.390	8.5
C6-C7	1.390	1.405	-1.1	1.393	-0.9
C7-C8	1.391	1.381	0.7	1.390	0.7
C8-C8a	1.392	1.407	-1.1	1.393	-1.0
C8a-C1	1.529	1.503	1.7	1.495	-0.5
C8a-C4a	1.409	1.429	-1.4	1.405	-1.7
C-H Bond					
C5-H11	1.080	1.081	-0.1	1.080	-0.1
C6-H12	1.081	1.083	-0.2	1.081	-0.2
C7-H13	1.081	1.083	-0.2	1.081	-0.2
C8-H14	1.080	1.081	-0.1	1.080	-0.1
C=O Bond					
C1=O9	1.200	1.241	-3.3	1.215	-2.1
C4=O10	1.200	1.241	-3.3	1.215	-2.1

	Singlet	Anion		Triplet	
C-C-C Angle			% Change		% Change
C1-C2-C3	129.4	130.6	-0.9	122.8	-6.0
C2-C3-C4	129.4	130.6	-0.9	122.8	-6.0
C3-C4-C4a	107.2	105.5	1.6	116.4	10.3
C4-C4a-C8a	123.4	123.9	-0.4	120.9	-2.4
C4-C4a-C5	117.0	117.4	-0.3	119.3	1.6
C4a-C8a-C1	123.4	123.9	-0.4	120.9	-2.4
C4a-C5-C6	120.4	121.6	-1.0	119.9	-1.4

C5-C6-C7	120.0	119.8	0.2	120.2	0.3
C6-C7-C8	120.0	119.8	0.2	120.2	0.3
C7-C8-C8a	120.4	121.6	-1.0	119.9	-1.4
C8-C8a-C1	117.0	117.4	-0.3	119.3	1.6
C8-C8a-C4a	119.6	118.6	0.8	119.9	1.1
C8a-C4a-C4	123.4	123.9	-0.4	120.9	-2.4
C8a-C4a-C5	119.6	118.6	0.8	119.9	1.1
C8a-C1-C2	107.2	105.5	1.6	116.4	10.3
C-C-H Angle					
C4a-C5-H11	118.5	117.2	1.1	118.8	1.4
C6-C5-H11	121.0	121.2	-0.2	121.2	0.0
C5-C6-H12	119.7	120.0	-0.3	119.8	-0.2
C7-C6-H12	120.2	120.2	0.0	120.0	-0.2
C6-C7-H13	120.2	120.2	0.0	120.0	-0.2
C8-C7-H13	119.7	120.0	-0.3	119.8	-0.2
C7-C8-H14	121.0	121.2	-0.2	121.2	0.0
C8a-C8-H14	118.5	117.2	1.1	118.8	1.4
C-C=O Angle					
C2-C1-O9	129.3	130.9	-1.2	120.2	-8.2
C8a-C1-O9	123.6	123.7	-0.1	123.5	-0.2
C3-C4-O10	129.3	130.9	-1.2	120.2	-8.2
C4a-C4-O10	123.6	123.7	-0.1	123.5	-0.2

Table S6: B3LYP/6-311g++(2d,2p) interatomic bond lengths (Å) and bond angles (deg.) for benzene radical anions and the corresponding to neutral S_0 and T_1 states. The major changes in bond lengths are shown in red.

	Singlet	Anion		Triplet	
C-C Bond			% Change		% Change
C1-C2	1.392	1.392	0.0	1.384	-0.6
C2-C3	1.392	1.392	0.0	1.384	-0.6
C3-C4	1.392	1.392	0.0	1.518	9.1
C4-C5	1.392	1.392	0.0	1.384	-0.6
C5-C6	1.392	1.392	0.0	1.384	-0.6
C6-C1	1.392	1.392	0.0	1.518	9.1
C-H Bond					
C1-H7	1.082	1.085	0.3	1.079	-0.6
C2-H8	1.082	1.085	0.3	1.083	-0.2
C3-H9	1.082	1.085	0.3	1.079	-0.6
C4-H10	1.082	1.085	0.3	1.079	-0.6

C5-H11	1.082	1.085	0.3	1.083	-0.2
C6-H12	1.082	1.085	0.3	1.079	-0.6

	Singlet	Anion		Triplet	
C-C-C Angle			% Change		% Change
C1-C2-C3	120.0	120.0	0.0	121.2	-0.4
C2-C3-C4	120.0	120.0	0.0	119.4	-0.4
C3-C4-C5	120.0	120.0	0.0	119.4	0.9
C4-C5-C6	120.0	120.0	0.0	121.2	-0.4
C5-C6-C1	120.0	120.0	0.0	119.4	-0.4
C6-C1-C2	120.0	120.0	0.0	119.4	0.9
C-C-H Angle					
C2-C1-H7	120.0	120.0	0.0	121.4	1.2
C6-C1-H7	120.0	120.0	0.0	119.2	-0.7
C1-C2-H8	120.0	120.0	0.0	119.4	-0.5
C3-C2-H8	120.0	120.0	0.0	119.4	-0.5
C2-C3-H9	120.0	120.0	0.0	121.4	1.2
C4-C3-H9	120.0	120.0	0.0	119.2	-0.7
C3-C4-H10	120.0	120.0	0.0	119.2	-0.7
C5-C4-H10	120.0	120.0	0.0	121.4	1.2
C4-C5-H11	120.0	120.0	0.0	119.4	-0.5
C6-C5-H11	120.0	120.0	0.0	119.4	-0.5
C5-C6-H12	120.0	120.0	0.0	121.4	1.2
C1-C6-H12	120.0	120.0	0.0	119.2	-0.7

Table S7: B3LYP/6-311g++(2d,2p) interatomic bond lengths (Å) and bond angles (deg.) for naphthalene radical anions and the corresponding to neutral S_0 and T_1 states. The major changes in bond lengths are shown in red.

	Singlet	Anion		Triplet	
C-C Bond			% Change		% Change
C1-C2	1.371	1.405	-2.4	1.438	
C2-C3	1.413	1.389	1.7	1.358	
C3-C4	1.371	1.405	-2.4	1.438	
C4-C4a	1.418	1.419	0.0	1.405	
C4a-C5	1.418	1.419	0.0	1.405	
C5-C6	1.371	1.405	-2.4	1.438	
C6-C7	1.413	1.389	1.7	1.358	
C7-C8	1.371	1.405	-2.4	1.438	
C8-C9	1.418	1.419	0.0	1.406	
C8a-C1	1.418	1.419	0.0	1.406	
C8a-C4a	1.429	1.448	-1.3	1.446	
C-H Bond					
C1-H9	1.082	1.085	-0.3	1.082	-0.3
C2-H10	1.081	1.084	-0.3	1.081	-0.3
C3-H11	1.081	1.084	-0.3	1.081	-0.3
C4-H12	1.082	1.085	-0.3	1.082	-0.3
C5-H13	1.082	1.085	-0.3	1.082	-0.3
C6-H14	1.081	1.084	-0.3	1.081	-0.3
C7-H15	1.081	1.084	-0.3	1.081	-0.3
C8-H16	1.082	1.085	-0.3	1.082	-0.3

	Singlet	Anion		Triplet	
C-C-C Angle			% Change		% Change
C1-C2-C3	120.3	120.1		119.9	
C2-C3-C4	120.3	120.1		119.9	
C3-C4-C4a	120.9	121.6		121.4	
C4-C4a-C8a	118.8	118.4		118.6	
C4-C4a-C5	122.3	123.2		122.8	
C4a-C8a-C1	118.8	118.4		118.6	
C4a-C5-C6	120.9	121.6		121.4	
C5-C6-C7	120.3	120.1		119.9	
C6-C7-C8	120.3	120.1		119.9	
C7-C8-C8a	120.9	121.6		121.4	
C8-C8a-C1	122.3	123.2		122.8	
C8-C8a-C4a	118.8	118.4		118.6	
C8a-C4a-C5	118.8	118.4		118.6	

C8a-C1-C2	120.9	121.6	121.4
C-C-H Angle			
C2-C1-H9	120.3	119.9	119.4
C8a-C1-H9	118.8	118.6	119.1
C1-C2-H10	120.1	119.8	119.3
C3-C2-H10	119.6	120.1	120.8
C2-C3-H11	119.6	120.1	120.8
C4-C3-H11	120.1	119.8	119.3
C3-C4-H12	120.3	119.9	119.4
C4a-C4-H12	118.8	118.6	119.1
C4a-C5-H13	118.8	118.6	119.1
C6-C5-H13	120.3	119.9	119.4
C5-C6-H14	120.1	119.8	119.3
C7-C6-H14	119.6	120.1	120.8
C6-C7-H15	119.6	120.1	120.8
C8-C7-H15	120.1	119.8	119.3
C7-C8-H16	120.3	119.9	119.4
C8a-C8-H16	118.8	118.6	119.1

Table S8: B3LYP/6-311g++(2d,2p) interatomic bond lengths (Å) and bond angles (deg.) for 1,2-DD-Bz radical anions and the corresponding neutral S_0 and T_1 states. The major changes in bond lengths are shown in red.

	Singlet	Anion		Triplet	
C-C Bond			% Change		% Change
C1-C2	1.381	1.398	-1.2	1.373	-1.8
C2-C3	1.241	1.343	-7.6	1.393	3.7
C3-C4	1.381	1.398	-1.2	1.373	-1.8
C4-C5	1.408	1.404	0.3	1.402	-0.1
C5-C6	1.403	1.396	0.5	1.389	-0.5
C6-C1	1.408	1.404	0.3	1.402	-0.1
C-H Bond					
C1-H7	1.079	1.090	-1.0	1.083	-0.6
C4-H8	1.079	1.090	-1.0	1.083	-0.6
C5-H9	1.083	1.088	-0.5	1.082	-0.6
C6-H10	1.083	1.088	-0.5	1.082	-0.6
	Singlet	Anion		Triplet	
C-C-C Angle			% Change		% Change
C1-C2-C3	127.2	121.2	5.0	121.0	-0.2
C2-C3-C4	127.2	121.2	5.0	121.0	-0.2
C3-C4-C5	110.4	118.9	-7.1	118.6	-0.3
C4-C5-C6	122.4	119.8	2.1	120.4	0.5
C6-C6-C1	122.4	119.8	2.1	120.4	0.5
C6-C1-C2	110.4	118.9	-7.1	118.6	-0.3
C-C-H Angle					
C6-C1-H7	122.6	118.5	3.5	120.8	1.9
C2-C1-H7	127.1	122.5	3.8	120.7	-1.5
C3-C4-H8	127.1	122.5	3.8	120.7	-1.5
C5-C4-H8	122.6	118.5	3.5	120.8	1.9
C4-C5-H9	118.7	120.3	-1.3	119.5	-0.7
C6-C5-H9	118.9	119.9	-0.8	120.1	0.2
C5-C6-H10	118.9	119.9	-0.8	120.1	0.2
C1-C6-H10	118.7	120.3	-1.3	119.5	-0.7

Table S9: B3LYP/6-311g++(2d,2p) interatomic bond lengths (Å) and bond angles (deg.) for 1,3-DD-Bz radical anions and the corresponding neutral S_0 and T_1 states. The major changes in bond lengths are shown in red.

	Singlet	Anion	
C-C Bond			% Change
C1-C2	1.378	1.402	-1.7
C2-C3	1.378	1.402	-1.7
C3-C4	1.375	1.391	-1.2
C4-C5	1.400	1.399	0.1
C5-C6	1.400	1.399	0.1
C6-C1	1.375	1.391	-1.2
C-H Bond			
C2-H7	1.094	1.086	0.7
C4-H8	1.081	1.089	-0.7
C5-H9	1.083	1.092	-0.8
C6-H10	1.081	1.089	-0.7
	Singlet	Anion	
C-C-C Angle			% Change
C1-C2-C3	115.0	117.9	-2.5
C2-C3-C4	125.0	121.0	3.3
C3-C4-C5	116.8	121.0	-3.5
C4-C5-C6	121.4	118.1	2.8
C5-C6-C1	116.8	121.0	-3.5
C6-C1-C2	125.0	121.0	3.3
C1-C2-H7	122.5	121.1	1.2
C3-C2-H7	122.5	121.1	1.2
C3-C4-H8	122.4	120.1	1.9
C5-C4-H8	120.8	118.9	1.6
C4-C5-H9	119.3	121.0	1.4
C6-C5-H9	119.3	121.0	1.4
C5-C6-H10	120.8	118.9	1.6
C1-C6-H10	122.4	120.1	1.9

Table S10: B3LYP/6-311g++(2d,2p) interatomic bond lengths (Å) and bond angles (deg.) for 1,4-DD-Bz radical anions and the corresponding neutral S_0 and T_1 states. The major changes in bond lengths are shown in red.

	Singlet	Anion	
C-C Bond			% Change
C1-C2	1.339	1.381	-3.0
C2-C3	1.480	1.430	3.5
C3-C4	1.339	1.381	-3.0
C4-C5	1.339	1.381	-3.0
C5-C6	1.480	1.430	3.5
C6-C1	1.339	1.381	-3.0
C-H Bond			
C2-H7	1.079	1.089	0.9
C3-H8	1.079	1.089	0.9
C4-H9	1.079	1.089	0.9
C5-H10	1.079	1.089	0.9
	Singlet	Anion	
C-C-C Angle			% Change
C1-C2-C3	117.2	121.4	-3.5
C2-C3-C4	117.2	121.4	-3.5
C3-C4-C5	125.6	117.2	7.2
C4-C5-C6	117.2	121.4	-3.5
C5-C6-C1	117.2	121.4	-3.5
C6-C1-C2	125.6	117.2	7.2
C-C-H Angle			
C1-C2-H8	127.9	122.0	4.8
C3-C2-H8	114.9	116.6	1.5
C2-C3-H9	114.9	116.6	1.5
C4-C3-H9	127.9	122.0	4.8
C3-C4-H10	127.9	122.0	4.8
C5-C4-H10	114.9	116.6	1.5
C4-C5-H11	114.9	116.6	1.5
C6-C5-H11	127.9	122.0	4.8

Table S11: B3LYP/6-311g++(2d,2p) interatomic bond lengths (Å) and bond angles (deg.) for 2,3-DD-Nh radical anions and the corresponding neutral S_0 and T_1 states. The major changes in bond lengths are shown in red.

	Singlet	Anion		Triplet	
C-C Bond			% Change		% Change

C1-C2	1.359	1.376	-1.2	1.398	1.6
C2-C3	1.251	1.359	-7.9	1.340	-1.4
C3-C4	1.359	1.376	-1.2	1.398	1.6
C4-C4a	1.439	1.428	0.7	1.439	0.8
C4a-C5	1.419	1.418	0.1	1.397	-1.5
C5-C6	1.371	1.376	-0.4	1.398	1.6
C6-C7	1.412	1.413	-0.1	1.388	-1.8
C7-C8	1.371	1.376	-0.4	1.398	1.6
C8-C9	1.419	1.418	0.1	1.397	-1.5
C8a-C1	1.439	1.428	0.7	1.439	0.8
C8a-C4a	1.443	1.436	0.5	1.425	-0.8
C-H Bond					
C1-H9	1.080	1.091	-1.0	1.087	-0.4
C4-H10	1.080	1.091	-1.0	1.087	-0.4
C5-H11	1.082	1.085	-0.3	1.082	-0.3
C6-H12	1.081	1.084	-0.3	1.081	-0.3
C7-H13	1.081	1.084	-0.3	1.081	-0.3
C8-H14	1.082	1.085	-0.3	1.082	-0.3

	Singlet	Anion		Triplet	
C-C-C Angle			% Change		% Change
C1-C2-C3	128.0	121.7	5.1	121.3	-0.3
C2-C3-C4	128.0	121.7	5.1	121.3	-0.3
C3-C4-C4a	111.0	119.6	-7.2	120.3	0.6
C4-C4a-C8a	121.0	118.7	1.9	118.4	-0.3
C4-C4a-C5	120.6	123.0	-2.0	122.5	-0.4
C4a-C8a-C1	121.0	118.7	1.9	118.4	-0.3
C4a-C5-C6	121.2	121.8	-0.5	120.9	-0.7
C5-C6-C7	120.3	119.9	0.3	120.0	0.1
C6-C7-C8	120.3	119.9	0.3	120.0	0.1
C7-C8-C8a	121.2	121.8	-0.5	120.9	-0.7
C8-C8a-C1	120.6	123.0	-2.0	122.5	-0.4
C8-C8a-C4a	118.5	118.4	0.1	119.1	0.6
C8a-C4a-C5	118.5	118.4	0.1	119.1	0.6
C8a-C1-C2	111.0	119.6	-7.2	120.3	0.6
C-C-H Angle					
C2-C1-H9	127.7	123.2	3.7	122.4	-0.6
C8a-C1-H9	121.2	117.2	3.4	117.2	0.0
C3-C4-H10	127.7	123.2	3.7	122.4	-0.6
C4a-C4-H10	121.2	117.2	3.4	117.2	0.0
C4a-C5-H11	118.6	118.2	0.3	119.2	0.8

C6-C5-H11	120.2	120.0	0.2	119.9	-0.1
C5-C6-H12	120.0	120.3	-0.2	119.9	-0.3
C7-C6-H12	119.7	119.9	0.2	120.2	0.3
C6-C7-H13	119.7	119.9	0.2	120.2	0.3
C8-C7-H13	120.0	120.3	-0.2	119.9	-0.3
C7-C8-H14	120.2	120.0	0.2	119.9	-0.1
C8a-C8-H14	118.6	118.2	0.3	119.2	0.8

Table S12: B3LYP/6-311g++(2d,2p) interatomic bond lengths (Å) and bond angles (deg.) for 1,2-DD-Nh radical anions and the corresponding neutral S_0 and T_1 states. The major changes in bond lengths are shown in red.

	Singlet	Anion	
C-C Bond			% Change
C1-C2	1.231	1.325	-7.1
C2-C3	1.401	1.416	-1.1
C3-C4	1.385	1.383	0.1
C4-C4a	1.431	1.418	0.9
C4a-C5	1.416	1.418	-0.1
C5-C6	1.375	1.375	0.0
C6-C7	1.409	1.414	-0.4
C7-C8	1.375	1.376	-0.1
C8-C9	1.407	1.420	-0.9
C8a-C1	1.404	1.422	-1.3
C8a-C4a	1.453	1.446	-0.5
C-H Bond			
C3-H9	1.079	1.089	-0.9
C4-H10	1.083	1.087	-0.4
C5-H11	1.082	1.086	-0.4
C6-H12	1.081	1.084	-0.3
C7-H13	1.081	1.084	-0.3
C8-H14	1.080	1.083	-0.3

	Singlet	Anion	
C-C-C Angle			% Change
C1-C2-C3	128.0	121.8	5.1
C2-C3-C4	110.6	119.5	-7.4
C3-C4-C4a	123.3	120.5	2.3
C4-C4a-C8a	121.0	118.5	2.1
C4-C4a-C5	121.7	122.5	-0.7
C4a-C8a-C1	109.7	118.2	-7.2

C4a-C5-C6	121.2	121.4	-0.2
C5-C6-C7	120.7	119.9	-0.7
C6-C7-C8	120.6	120.1	0.4
C7-C8-C8a	120.0	122.0	0.0
C8-C8a-C1	130.0	124.2	4.7
C8-C8a-C4a	120.3	117.6	2.3
C8a-C4a-C5	117.3	119.0	-1.4
C8a-C1-C2	127.3	121.5	4.8
C-C-H Angle			
C2-C3-H9	126.6	122.0	3.8
C4-C3-H9	122.8	118.5	3.6
C3-C4-H10	118.8	120.8	-1.7
C4a-C4-H10	117.9	118.7	-0.7
C4a-C5-H11	118.9	118.7	-0.2
C6-C5-H11	119.9	119.9	0.0
C5-C6-H12	119.8	120.2	-0.3
C7-C6-H12	119.5	119.9	-0.3
C6-C7-H13	119.6	119.7	-0.1
C8-C7-H13	119.8	120.3	-0.4
C7-C8-H14	120.9	120.8	0.1
C8a-C8-H14	119.1	117.2	1.6

Table S13: Calculated dipole moments of the *p*-BQ, 2,3-DD-*p*-BQ, 1,4-NQ, and 2,3-DD-1,4-NQ radical anions. Only the B3LYP/6-311g++(2d,2p) results are shown.

	Dipole Moment (Debye)		
Molecule	Anion	Parent	Triplet
p-BQ	0.00090	0.00030	0.00160
2,3-DD-*p*-BQ	2.14770	2.37600	3.24900
1,4-NQ	3.32290	1.45640	3.16714
2,3-DD-1,4-NQ	5.23790	3.97260	3.77890

Table S14: Normal harmonic vibrational modes (ν_1 to ν_{24}) for the anion, neutral singlet and the T_1 state in 2,3-didehydro-*p*-BQ.

Mode	Anion	Singlet	Triplet
ν_1	3160.5	3204.6	3198.1
ν_2	3139.6	3187.1	3189.2

v_3	2014.1	2115.0	2074.2
v_4	1584.2	1774.0	1525.4
v_5	1526.2	1760.0	1467.1
v_6	1477.3	1625.0	1342.5
v_7	1343.6	1332.3	1324.7
v_8	1158.8	1203.4	1181.0
v_9	1128.7	1053.4	1098.0
v_{10}	985.9	1018.5	989.4
v_{11}	896.4	976.4	906.4
v_{12}	885.6	855.3	784.4
v_{13}	794.0	842.3	771.3
v_{14}	767.6	753.8	723.2
v_{15}	743.5	727.8	565.2
v_{16}	636.7	708.9	562.6
v_{17}	613.7	607.0	485.4
v_{18}	564.4	565.4	461.4
v_{19}	481.6	465.8	454.0
v_{20}	420.5	429.5	435.5
v_{21}	412.6	388.0	360.5
v_{22}	379.9	359.8	225.1
v_{23}	278.1	139.9	200.6
v_{24}	121.6	88.3	85.3

Table S15: Normal harmonic vibrational modes (v_1 to v_{30}) for the anion, neutral singlet and the T_1 state in *p*-BQ.

Mode	Anion	Singlet	Triplet
v_1	3149.9	3193.2	3750.7
v_2	3144.8	3190.8	3210.9
v_3	3124.9	3175.2	3209.2
v_4	3124.4	3175.0	3195.7

v_5	1640.4	1727.0	3135.7
v_6	1529.1	1726.0	1610.1
v_7	1495.8	1677.0	1536.3
v_8	1485.0	1642.6	1442.3
v_9	1448.6	1400.0	1391.5
v_{10}	1374.3	1392.2	1368.7
v_{11}	1268.8	1316.9	1240.9
v_{12}	1217.4	1239.3	1202.8
v_{13}	1156.3	1171.1	1191.7
v_{14}	1076.7	1086.3	1020.9
v_{15}	970.1	1044.6	951.0
v_{16}	965.7	1034.6	915.1
v_{17}	962.7	954.0	843.6
v_{18}	864.0	918.3	816.4
v_{19}	819.6	824.6	814.4
v_{20}	792.6	770.9	806.9
v_{21}	770.9	763.7	772.1
v_{22}	768.3	755.3	621.8
v_{23}	631.8	603.3	583.5
v_{24}	516.8	517.5	526.7
v_{25}	475.1	460.0	479.6
v_{26}	471.5	456.9	443.1
v_{27}	401.6	414.8	389.4
v_{28}	391.4	342.7	388.7
v_{29}	317.8	239.7	295.6
v_{30}	128.9	92.7	121.7

Table S16: Normal harmonic vibrational modes (v_1 to v_{48}) for the anion, neutral singlet and the T_1 state in 1,4-NQ.

Mode	Anion	Singlet	Triplet
v_1	3186.3	3207.5	3211.1
v_2	3183.6	3204.5	3204.1
v_3	3159.4	3196.6	3196.1

v_4	3155.8	3191.2	3193.0
v_5	3137.7	3179.1	3187.0
v_6	3136.4	3177.3	3176.5
v_7	1627.9	1721.1	1629.3
v_8	1619.7	1715.6	1579.6
v_9	1549.3	1660.0	1569.0
v_{10}	1537.6	1627.9	1497.7
v_{11}	1488.8	1608.9	1476.5
v_{12}	1467.9	1508.4	1463.9
v_{13}	1459.3	1489.3	1414.3
v_{14}	1419.6	1398.7	1342.7
v_{15}	1342.0	1353.1	1320.6
v_{16}	1320.9	1313.0	1268.3
v_{17}	1241.4	1312.4	1220.8
v_{18}	1236.0	1252.4	1183.2
v_{19}	1173.3	1188.3	1175.6
v_{20}	1140.5	1165.0	1148.8
v_{21}	1139.7	1134.8	1091.3
v_{22}	1092.4	1081.8	1079.9
v_{23}	1062.2	1071.5	1063.5
v_{24}	1029.7	1034.7	1016.0
v_{25}	991.1	1034.3	1013.0
v_{26}	983.3	1025.9	980.1
v_{27}	941.3	1004.9	918.2
v_{28}	883.8	927.0	890.5
v_{29}	836.2	885.7	829.3
v_{30}	807.5	836.2	805.7
v_{31}	804.9	793.1	775.1

v_{32}	769.4	780.9	754.6
v_{33}	762.3	767.8	750.6
v_{34}	711.0	703.6	709.2
v_{35}	673.6	701.3	634.4
v_{36}	618.6	612.3	575.8
v_{37}	603.3	599.7	560.8
v_{38}	560.3	554.2	537.1
v_{39}	480.5	480.2	472.6
v_{40}	467.7	453.2	455.6
v_{41}	463.2	451.9	436.7
v_{42}	427.4	416.9	417.1
v_{43}	362.8	373.8	334.3
v_{44}	337.5	267.0	308.6
v_{45}	267.6	266.9	260.4
v_{46}	192.5	184.6	187.5
v_{47}	134.7	120.7	130.7
v_{48}	106.9	78.2	95.4

Table S17: Normal harmonic vibrational modes (v_1 to v_{42}) for the anion, neutral singlet and T_1 state in 2,3-didehydro-1,4-NQ.

Mode	Anion	Singlet	Triplet
v_1	3187.5	3208.8	3209.0

v_2	3184.6	3205.4	3205.9
v_3	3159.4	3194.2	3194.1
v_4	3140.5	3181.0	3180.9
v_5	2006.3	2126.6	1697.3
v_6	1613.6	1770.6	1688.2
v_7	1597.5	1759.5	1650.5
v_8	1551.2	1613.1	1619.8
v_9	1544.1	1605.2	1604.6
v_{10}	1469.3	1490.7	1502.4
v_{11}	1449.0	1476.7	1484.2
v_{12}	1329.3	1340.3	1348.7
v_{13}	1269.7	1293.2	1301.1
v_{14}	1190.2	1188.5	1231.2
v_{15}	1178.3	1175.6	1223.8
v_{16}	1101.8	1158.3	1186.9
v_{17}	1095.5	1086.2	1116.9
v_{18}	1054.8	1066.9	1072.4
v_{19}	1042.5	1023.9	1061.4
v_{20}	985.0	1007.7	1026.9
v_{21}	976.9	1001.8	1026.7
v_{22}	976.2	966.0	1004.6
v_{23}	870.9	921.8	925.5
v_{24}	827.5	812.7	813.1
v_{25}	768.7	804.8	792.3
v_{26}	758.2	793.6	791.7
v_{27}	708.9	716.3	732.2
v_{28}	664.4	699.5	698.9
v_{29}	652.8	662.9	684.3

v_{30}	615.2	657.3	673.7
v_{31}	573.4	565.4	569.3
v_{32}	533.0	540.1	541.0
v_{33}	476.3	484.0	475.1
v_{34}	457.6	438.2	434.7
v_{35}	443.5	431.0	428.2
v_{36}	419.1	420.1	417.1
v_{37}	353.0	362.4	334.9
v_{38}	310.9	276.4	262.9
v_{39}	274.1	210.2	254.7
v_{40}	190.2	190.4	184.9
v_{41}	135.6	104.7	120.1
v_{42}	104.5	79.2	66.4

References

1. R. S. Ruoff, K. M. Kadish, P. Boulas and E. C. M. Chen, *J. Phys. Chem. A*, 1995, **99**, 8843.
2. X.-Q. Zhu and C.-H. Wang, *J. Org. Chem.*, 2010, **75**, 5037.
3. J. Calbo, R. Viruela, E. Ortí and J. Aragó, *Chem.Phys.Chem.*, 2016, **17**, 3881.
4. M. J. Frisch, G. W. Trucks, H. B. Schlegel, G. E. Scuseria, M. A. Robb, J. R. Cheeseman, G. Scalmani, V. Barone, B. Mennucci, G. A. Petersson, H. Nakatsuji, M. Caricato, X. Li, H. P. Hratchian, A. F. Izmaylov, J. Bloino, G. Zheng, J. L. Sonnenberg, M. Hada, M. Ehara, K. Toyota, R. Fukuda, J. Hasegawa, M. Ishida, T. Nakajima, Y. Honda, O. Kitao, H. Nakai, T. Vreven, J. A. Montgomery, Jr., J. E. Peralta, F. Ogliaro, M. Bearpark, J. J. Heyd, E. Brothers, K. N. Kudin, V. N. Staroverov, R. Kobayashi, J. Normand, K. Raghavachari, A. Rendell, J. C. Burant, S. S. Iyengar, J. Tomasi, M. Cossi, N. Rega, N. J. Millam, M. Klene, J. E. Knox, J. B. Cross, V. Bakken, C. Adamo, J. Jaramillo, R. Gomperts, R. E. Stratmann, O. Yazyev, A. J. Austin, R. Cammi, C. Pomelli, J. W. Ochterski, R. L. Martin, K. Morokuma, V. G. Zakrzewski, G. A. Voth, P. Salvador, J. J. Dannenberg, S. Dapprich, A. D. Daniels, Ö. Farkas, J. B. Foresman, J. V. Ortiz, J. Cioslowski and D. J. Fox, Wallingford, CT, 2009.